Research Square

Preprints are preliminary reports that have not undergone peer review.
They should not be considered conclusive, used to inform clinical practice,
or referenced by the media as validated information.

EGCG targeting JAK1/ STAT5 or STAT6 dampens pseudorabies virus replication via inhibiting BNIP3/caspase-3-dependent apoptosis

Changchao Huan

changchaohuan@yzu.edu.cn

Yangzhou University

Weiyin Xu
Jinghua Cheng
Jianbin Wang
Ping Yan
Luyao Jiang
Song Gao

Article

Keywords: PRV, EGCG, STATs, BNIP3, apoptosis

Posted Date: September 25th, 2026

DOI: https://doi.org/10.21203/rs.3.rs-10749480/v1

License: This work is licensed under a Creative Commons Attribution 4.0 International License.
Read Full License

Additional Declarations: There is **NO** Competing Interest.

EGCG targeting JAK1/ STAT5 or STAT6 dampens pseudorabies virus replication via inhibiting BNIP3/caspase-3-dependent apoptosis

Weiyin Xu[1,2,3#], Jinghua Cheng[4#], Jianbin Wang[1,2,3#], Ping Yan[1,2,3], Luyao Jiang[1,2,3] and Song Gao[1,2,3], Changchao Huan[1,2,3]*.

[1] Institute of Agricultural Science and Technology Development, College of Veterinary Medicine, Yangzhou University, Yangzhou, China.

[2] Jiangsu Co-Innovation Center for Prevention and Control of Important Animal Infectious Diseases and Zoonoses, Yangzhou, China.

[3] Key Laboratory of Avian Bioproduct Development, Ministry of Agriculture and Rural Affairs, Yangzhou, China.

[4] Institute of Animal Sciences and Veterinary Medicine, Shanghai Academy of Agricultural Sciences, Shanghai 201106.

* Correspondence: changchaohuan@yzu.edu.cn.

[#] These authors have contributed equally to this work.

Abstract:

Our previous study demonstrated that epigallocatechin gallate (EGCG) suppresses the pseudorabies virus (PRV) replication. In this study, we found that PRV replication triggers caspase-3-dependent apoptosis. Further investigation revealed that BNIP3 enhances this apoptotic process, facilitating PRV propagation. Mechanistically, PRV infection upregulates JAK1 expression and induces phosphorylation of STAT1, STAT5, and STAT6, while concurrently suppressing STAT3 phosphorylation. Intriguingly, JAK1, STAT3, STAT5, and STAT6 collectively promote BNIP3/caspase-3-mediated apoptosis to enhance viral replication, whereas STAT1 exerts an opposing effect by inhibiting this apoptotic pathway. Notably, EGCG attenuates PRV-induced apoptosis, thereby impairing viral replication. Specifically, EGCG downregulates PRV-mediated

expression of JAK1, BNIP3, and phosphorylation of STAT1, STAT5, and STAT6, while restoring the diminished phosphorylation of STAT3. These findings indicate that EGCG inhibits apoptosis primarily through the JAK1/STAT5 and JAK1/STAT6 pathways, rather than the JAK1/STAT1 or JAK1/STAT3 pathways, to suppress PRV replication.This study provides new insights into the molecular mechanisms of PRV-induced apoptosis and highlights the therapeutic potential of EGCG in mitigating PRV infection.

Keywords: PRV, EGCG, STATs, BNIP3, apoptosis

Introduction

Pseudorabies virus (PRV), the causative agent of Aujeszky's disease, is an alphaherpesvirus characterized by a double-stranded DNA genome. As a member of this subfamily that includes herpes simplex virus types 1 (HSV-1) and 2 (HSV-2) as well as varicella-zoster virus [1-3]. PRV has served as an important model organism for studying alphaherpesvirus biology and latency mechanisms. In its natural porcine hosts, PRV infection typically manifests as neuroencephalitis accompanied by respiratory and reproductive disorders, posing significant economic burdens in endemic regions worldwide. Notably, since 2012, the emergence of novel PRV variants [4, 5], has complicated disease control efforts, as these strains demonstrate reduced susceptibility to existing vaccination strategies. Particularly, recent reports from China documenting PRV's zoonotic potential, with clinical cases of human endophthalmitis and viral isolation from cerebrospinal fluid [6-9], highlighting growing public health implications.

Apoptosis serves as a fundamental biological process that maintains cellular homeostasis and regulates organismal development [10-13]. This programmed cell death mechanism functions as a crucial host defense system against pathogens while playing pivotal roles in tissue development and cellular senescence. However, the relationship between alphaherpesviruses and apoptosis remains controversial, with studies demonstrating both pro- and anti-apoptotic effects. In the case of PRV, multiple apoptotic pathways have been identified. PRV has been shown to induce apoptosis through oxidative stress mechanisms [14], and via its gM protein, which triggers

mitochondria-related apoptosis [15]. Conversely, other studies have demonstrated that PRV infection activates apoptosis through the p38 MAPK and JNK/SAPK pathways [16] while the viral US3 protein exhibits anti-apoptotic effects by activating PI3K/AKT and NF-κB signaling [17]. The Janus kinase/signal transducer and activator of transcription (JAK/STAT) signaling pathway, known for its critical role in cell development [18], and its association with colorectal adenoma progression, represents the key regulatory network in cellular processes. Given these diverse findings and the importance of JAK/STAT signaling in cellular regulation, we specifically investigated its involvement in PRV-induced apoptosis.

Epigallocatechin-3-gallate (EGCG), the predominant bioactive polyphenol in nature, exhibits remarkable pleiotropic effects including antioxidant, antiviral, antibacterial, and anti-inflammatory properties, along with demonstrated antitumor and antiangiogenic activities [19-26].Our previous work established that EGCG exerts dose-dependent inhibition of PRV infection by disrupting viral adsorption, cellular entry, and replication processes [27]. Building on these findings, the current study investigates EGCG's potential to modulate PRV replication through regulation of apoptosis via the JAK1/STATs/BNIP3/caspase-3 signaling axis.

Material and methods

Cells and viruses

PK15 and PK15 B6 cells were obtained from the Yangzhou University laboratory and maintained in Dulbecco's modified Eagle medium containing 5% fetal bovine serum.

The PRV strain XJ5 (mutant strain) was isolated and stored at the Yangzhou University laboratory. PRV Ra strain (classic strain) was purchased from the China Institute of Veterinary Drug Control.

Antibodies and Reagents

The EGCG was purchased from Selleck. The JAK1 tyrosine kinase inhibitor Ruxolitinib (INCB018424) was acquired from APExBIO. The transfection reagent Fuguen was purchased from Progema. Anti-JAK1 was obtained from Cell Signaling

Technology. Anti-phospho-STAT1, anti-STAT1, anti-phospho-STAT3, anti-STAT3, anti-phospho-STAT5, anti-STAT5, anti-phospho-STAT6, and anti-STAT6 were procured from Affinity. The anti-BNIP3 was obtained from ABclonal. Anti-caspase-3 antibodies were acquired from Santa Cruz. Bax and Cytochrome C were purchased from Proteintech. Anti-β-actin was obtained from TransGen Biotech. The gE and UL42 antibodies were obtained from our laboratory. Caspase-3 Activity Assay Kit was from Beyotime. Apoptosis Assays Kit was purchased from UE.

Establishment of pcDNA3.1-BNIP3 plasmid and transfection

The porcine BNIP3 sequence was downloaded from NCBI, and the primers were designed using Oligo 6 (Table S1). The PCR product was cloned into the pcDNA3.1 vector to generate pcDNA3.1-BNIP3. PK15 and PK15 B6 cells were transfected with 2.5 μg pcDNA3.1-BNIP3 using 7.5 μL Fugene. After 24 h of the transfection, the culture media was removed, changed with fresh media, and the cells were infected with PRV XJ5 and Ra. BNIP3 expression and other proteins change were detected using Western blot.

Generation of gene knockout cell lines via CRISPR/Cas9 system

Single Guide RNAs (sgRNAs) targeting porcine BNIP3, STAT1, STAT3, STAT5, and STAT6 (Table S1) were synthesized and cloned into the lentiCRISPR v2 vector. Human 293T cells were seeded in 4 cm dishes with 1×10^6 per dish. The cells were transfected with 1100 ng/dish sgRNA, 658 ng/dish pLP1, 309 ng/dish pLP2 (packaging plasmid), and 430 ng/dish pLPVSVG (envelope plasmid) using Fugene. After 24, 48, and 72 h of the transfection, the culture media containing lentivirus were collected and used to infect PK15 cells, which were then screened with puromycin (2 μg/mL) for three days. BNIP3, STAT1, STAT3, STAT5, and STAT6 expressions were determined using real-time quantitative polymerase chain reaction (RT-qPCR) and Western blot analysis.

Western blot

The cell samples were lysed with cell lysis buffer (Beyotime). BCA assay was used to detect protein concentrations. Equal amounts of proteins were separated using 12% SDS-PAGE, then transferred into the nitrocellulose membrane. The membrane

was blocked with 3% non-Fat powered milk for 2 h at room temperature (RT) and incubated overnight at 4℃ with different primary antibodies. After 24 h, membranes were incubated with secondary antibodies for 1.5 h at RT, and protein bands were analyzed using the Super ECL Reagent Solution kit (Shanghai share Biotechnology, China).

RT-qPCR

Total RNA was extracted with the TriZol reagent. For cDNA synthesis, 1 μg of total RNA was reverse-transcribed with HiScript III-RT SuperMix (+gDNA wiper) (Vazyme, China) for qPCR. cDNA was stored at -80 ℃. Gene expression was quantified using RT-qPCR with ChamQ Universal SYBR qPCR Master Mix (Vazyme, China). The data were normalized based on the β-actin expression level in each sample. The $2^{-\Delta\Delta Ct}$ method was used to calculate relative expression changes. The RT-qPCR primers for porcine BNIP3, STAT1, STAT3, STAT5, and STAT6 are listed in Table S2.

YF488-Annexin V (FITC)/PI double staining

The YF488-Annexin V and PI Apoptosis detection kit was used to determine apoptosis according to the manufacturer's instructions. After infection with PRV XJ5 and Ra (MOI = 0.1) for 24 h, the cells were digested with trypsin without EDTA. The cells were collected by centrifugation at 1,000 g for 5 min and washed two times with PBS. Furthermore, cells were suspended in a binding buffer and incubated with 5μL YF488-Annexin V and 5 μL PI staining at ice for 10 min for flow cytometry analysis.

Caspase-3 activity assay

Caspase-3 Activity Assay Kit was used to analyze cell apoptosis rate. The cell samples were digested with trypsin-EDTA and centrifuged at 600×g 4 ℃ for 5 min. The harvested cells were washed twice with PBS. Briefly, 200 μL cellular lysate was added to cells and incubated at 4 ℃ for 15 min. The lysate was then centrifuged at 12,000 rpm and 4 °C for 15 min to remove insoluble debris. After transferring the supernatant to a new centrifuge tube, 50 μL supernatant was mixed with 10 μL Ac-DEVD-pNA (2 mM) and 40 μL detection buffer. Caspase-3 enzymatic activity was finally quantified by measuring the absorbance at 450 nm with a microplate spectrophotometer.

Statistical analysis

All experiments were repeated at least three times independently, and all data were presented as mean ± SD. The data were analyzed using GraphPad Prism software (GraphPad Software, San Diego, CA). The differences were considered statistically significant when $P < 0.05$.

Results

PRV replication activates caspase-3-dependent apoptosis

To characterize PRV-induced apoptosis, PK15 and PK15-B6 cells were infected with PRV XJ5 and Ra strains at a multiplicity of infection (MOI) of 0.1. Infected cells were harvested at 6, 12, and 24 hours post-infection (hpi) for apoptosis assessment. Both mock-infected and PRV-infected cells were stained with Annexin V-FITC and propidium iodide (PI) [28] and subjected to flow cytometric analysis. As shown in the representative apoptosis profiles (Fig. 1A for PK15; Fig. S1A for PK15-B6), PRV infection significantly enhanced apoptotic rates compared to mock-infected controls. Results revealed that both XJ5 and Ra strains induced approximately 2.5-to 3-fold increases in apoptosis at 24 hpi across both cell lines. These results demonstrate that PRV infection triggers substantial apoptosis in porcine kidney epithelial cells within 24 h of infection.

To delineate the apoptotic pathway activated by PRV infection, we performed a time-course experiment in PK15 cells infected with PRV XJ5 and Ra strains (MOI = 0.1) for 2-24 h. Western blot analysis demonstrated the progressive downregulation of full-length procaspase-3 protein levels as late as 24 hpi, while protein levels of Bax and cytochrome C remained unchanged (Fig. 1B, C). suggesting selective activation of caspase-3-mediated apoptosis These preliminary observations indicate a selective activation of caspase-3-mediated apoptotic signaling, rather than full-scale mitochondrial apoptosis engagement. This caspase-3-dependent mechanism was consistently observed in PK15-B6 cell lines (Fig. S1B, C). Complementary enzymatic assays revealed the significant increase in caspase-3 activity at 24 hpi in both PK15 (Fig. 1D, E) and PK15-B6 cells (Fig. S1D, E). The temporal correlation between caspase-3 activation and apoptotic progression strongly indicates that PRV-induced

apoptosis primarily occurs through the caspase-3 pathway, independent of Bax/cytochrome C-mediated mitochondrial apoptosis.

BNIP3 promotes apoptosis during PRV replication

BNIP3 is a well-characterized pro-apoptotic protein localized to the mitochondrial outer membrane, where it mediates mitochondrial dysfunction and cell death [29-31]. While its role in various apoptotic pathways has been established, its involvement in PRV-induced apoptosis remained to be elucidated. Our time-course experiments revealed that PRV infection elicits significant, strain-independent upregulation of BNIP3 in both PK15 and PK15-B6 cell lines. In PK15 cells, BNIP3 protein accumulation was detected as early as 18 hours post-infection and further escalated through 24 hpi (Fig. 2A, B), while in PK15-B6 cells, BNIP3 upregulation was observed as early as 12 hpi and persisted through 24 hpi (Fig. S2A, B).

To investigate the potential regulatory role of BNIP3 in apoptosis during PRV infection, we conducted the experiment in which BNIP3 was overexpressed in PK15 cells for 24 h prior to infection with PRV strains XJ5 or Ra for an additional 24 h. Following this, western blot analysis and caspase-3 activity assays were performed. The results indicated that BNIP3 overexpression resulted in the reduction of caspase-3 expression (Fig. 2C, E) and the increase in caspase-3 enzymatic activity during PRV infection in PK15 cells (Fig. 2D, F). To corroborate these findings, similar experiments were conducted using PK15 B6 cells. The data from these experiments confirmed that BNIP3 overexpression led to decreased caspase-3 expression and elevated caspase-3 enzymatic activity during PRV replication in PK15 B6 cells (Fig. S2C-F).

Subsequently, we knocked out BNIP3 in PK15 cells using a lentivirus packaging system, and the knockout efficiency was examined by RT-qPCR and Western blotting. (Fig. 2G, H). The BNIP3-deficient cells were subsequently infected with PRV XJ5 for duration of 24 h. Western blot analysis demonstrated that knockout BNIP3 led to the upregulation of caspase-3 expression (Fig. 2H). And the caspase-3 activity assay indicated the reduction in enzyme activity during PRV infection (Fig. 2I). Consistent results were obtained when cells were infected with the PRV Ra strain (Fig. 2J, K). Furthermore, flow cytometry analysis revealed that knockout BNIP3 attenuated PRV

XJ5 and Ra-induced apoptosis (Fig. 2L). Collectively, these findings suggest that BNIP3 facilitates apoptosis induced by PRV XJ5 and Ra.

The effect of PRV infection on the JAK/STATs pathway.

The JAK/STATs signaling pathway plays a critical role in cell development [18], regulating various developmental processes and antiviral immunity [32, 33]. However, the impact of the JAK/STAT signaling pathway during PRV infection has not been thoroughly investigated. Hence, we sought to explore the effect of PRV replication on this signaling pathway. PK15 and PK15 B6 cells were infected with PRV XJ5 (MOI = 0.1) for 2, 4, 8, 12, 18, and 24 h. As depicted in Fig. 3A and S3A, PRV XJ5 infection led to an increase in JAK1 expression at 12, 18, and 24 h post-infection (hpi), along with the phosphorylation of STAT1, STAT5, and STAT6 at 18 and 24 hpi. However, phospho-STAT3 was reduced at 18 and 24 hpi. To ascertain whether this increase is strain-dependent, we also evaluated the effect of the PRV Ra strain on the JAK/STAT signaling pathway in PK15 and PK15-B6 cells. As expected, PRV Ra upregulated JAK1 expression at 12, 18, and 24 hpi, as well as the phosphorylation of STAT1, STAT5, and STAT6 at 18 and 24 hpi (Fig. 3B and S3B). Nevertheless, similar to PRV XJ5, PRV Ra also decreased phospho-STAT3 at 18 and 24 hpi.

STAT1 downregulated apoptosis induced by PRV.

To investigate the impact of STAT1 on apoptosis induced by PRV, we employed the lentivirus packaging system to knock out STAT1 in PK15 cells, which was confirmed through qRT-PCR and western blot analysis (Fig. 4A, B and D). Subsequently, the cells were infected with PRV XJ5 or Ra for 24 h. Western blot analysis revealed that STAT1 knockout resulted in increased BNIP3 expression and decreased caspase-3 levels (Fig. 4B, D). Moreover, the caspase-3 activity assay showed that STAT1 knockout led to increased caspase-3 enzyme activity during PRV infection (Fig. 4C, E). Additionally, flow cytometry analysis indicated that STAT1 knockout upregulated apoptosis induced by both PRV XJ5 and Ra (Fig. 4F, G). These results collectively suggest that STAT1 downregulates BNIP3/caspase-3-dependent apoptosis induced by PRV XJ5 and Ra.

STAT3 upregulated apoptosis induced by PRV.

To explore the influence of STAT3 on apoptosis induced by PRV, we employed the

Lentivirus packaging system to knock out STAT3 in PK15 cells, and the success of STAT3 gene knockout was confirmed using RT-qPCR and western blot analysis (Fig. 5A, B and D). Subsequently, the cells were infected with PRV XJ5 for 24 h. Western blot analysis revealed that STAT3 knockout led to an increase in caspase-3 expression and a decrease in BNIP3 levels (Fig. 5B). Additionally, the caspase-3 activity assay showed that STAT3 knockout decreased the enzyme activity of caspase-3 during PRV XJ5 infection (Fig. 5C). To determine whether the role of STAT3 is strain-dependent, we used PRV Ra to evaluate its impact. As expected, STAT3 knockout also resulted in increased caspase-3 expression and decreased BNIP3 levels during PRV Ra infection (Fig. 5D). Similarly, the caspase-3 activity assay revealed that STAT3 knockdown decreased caspase-3 enzyme activity during PRV Ra infection (Fig. 5E). Furthermore, flow cytometry analysis also indicated that STAT3 knockout reduced apoptosis induced by PRV XJ5 and Ra (Fig. 5F, G). These findings collectively suggest that STAT3 upregulates apoptosis induced by both PRV XJ5 and Ra.

STAT5 promoted apoptosis induced by PRV.

To explore the impact of STAT5 on apoptosis induced by PRV, we utilized the lentivirus packaging system to knock out STAT5 in PK15 cells, and the success of STAT5 gene knockout was confirmed using RT-qPCR and western blot analysis (Fig. 6A, B and D). Subsequently, the cells were infected with either PRV XJ5 or Ra for 24 h. Western blot analysis revealed that STAT5 knockout inhibited UL42 expression and led to an increase in caspase-3 expression, while reducing BNIP3 levels (Fig. 6B, D). Additionally, the caspase-3 activity assay confirmed that STAT5 knockout reduced the enzyme activity of caspase-3 during PRV XJ5 or Ra infection (Fig. 6C, E). Furthermore, flow cytometry analysis indicated that STAT5 knockout decreased apoptosis induced by PRV XJ5 or Ra (Fig. 6F, G). These findings indicate that STAT5 positively regulates apoptosis induced by both PRV XJ5 and Ra.

The effect of STAT6 in apoptosis induced by PRV

We utilized the lentivirus packaging system to knock out STAT6 in PK15 cells and investigate its role in apoptosis induced by PRV. The success of STAT6 gene knockout was confirmed through RT-qPCR and western blot analysis (Fig. 7A, B and D).

Subsequently, the cells were infected with either PRV XJ5 or Ra for 24 h. Western blot analysis revealed that STAT6 knockout increased caspase-3 expression while reducing BNIP3 levels and UL42 expression (Fig. 7B, D). The caspase-3 activity assay confirmed that STAT6 knockout decreased the enzyme activity of caspase-3 during PRV XJ5 or Ra infection (Fig. 7C, E). Furthermore, flow cytometry analysis showed that STAT6 knockout reduced apoptosis induced by PRV XJ5 or Ra (Fig.7F, G). These results provide evidence that STAT6 positively regulates apoptosis induced by both PRV XJ5 and Ra.

JAK1 upregulated apoptosis induced by PRV infection

The JAK/STAT pathway has been shown to influence cell apoptosis and mitochondrial injury in ischemia-reperfusion-induced kidney injury [34]. To investigate the role of JAK1/STATs in apoptosis during PRV infection, we treated the cells with the JAK1 inhibitor ruxolitinib. Interestingly, ruxolitinib treatment resulted in an increase in caspase-3 expression, a decrease in BNIP3 expression, and a reduction in the phosphorylation of STAT1, STAT5, and STAT6 during PRV XJ5 and Ra infection (Fig. 8A, B). Notably, it led to an increase in phospho-STAT3 levels. Furthermore, the JAK1 inhibitor ruxolitinib consistently inhibited the enzyme activity of caspase-3 during PRV XJ5 and Ra infection (Fig. 8C, D). These findings confirm that PRV infection activates the JAK1/STAT1, STAT5, and STAT6 signaling pathways, while inhibiting the JAK1/STAT3 signaling pathway to regulate BNIP3/caspase-3-dependent apoptosis.

EGCG inhibited apoptosis induced by PRV depending on JAK1/STAT5 or STAT6 pathway

PK15 and PK15 B6 cells were pretreated with EGCG (50 μM) for 1 h and infected PEV XJ5 or Ra with EGCG (50 μM) for 24 h to explore the role of EGCG in apoptosis induced by PRV. Flow cytometry revealed that EGCG decreased apoptosis induced by PRV XJ5 or Ra at PK15 and PK15 B6 cells (Fig. 9A and Fig.S4A). Caspase-3 activity assay confirmed that EGCG reduced the enzyme activity of caspase-3 during PRV XJ5 or Ra infected PK15 and PK15 B6 cells (Fig.9B, C and Fig.S4B, C). These results demonstrated that EGCG inhibited PRV replication by reducing PRV-induced apoptosis.

PPK15 and PK15 B6 cells were pretreated with EGCG (50 μM) for 1 h and

infected PEV XJ5 or Ra with EGCG (50 μM) for 24 h to study the role of EGCG in the JAK1/STATs pathway. Western blot analysis revealed that EGCG reduced JAK1, BNIP3, phospho-STAT1, phospho-STAT5, and phospho-STAT6 expressions induced by PRV XJ5 or Ra infection (Fig.9D, E and Fig.S4D, E). Nevertheless, EGCG promoted phospho-STAT3 decreased by PRV XJ5 or Ra (Fig.9D, E and Fig.S4D, E). These results confirmed that EGCG inhibited apoptosis via JAK1/STAT5 or STAT6 pathways but not by JAK1/STAT1 or STAT3 pathways.

Discussion

Apoptosis plays a crucial role in maintaining cellular homeostasis and survival [35-38]. Viral infections can directly induce apoptosis in host cells; for example, influenza virus proteins can trigger apoptosis in infected cells [39, 40], and respiratory syncytial virus clearance relies on apoptosis in bronchial epithelial cells [41]. Investigating the interplay between viruses and host cells, as well as the virus's pathogenesis, involves studying the relationship between virus infection and apoptosis. This study found that PRV infection-induced apoptosis in PK15 and PK15 B6 cells depended on caspase-3.

BNIP3 is a pro-apoptotic protein and combines with Bcl-2 to disintegrate Beclin-1, thereby promoting autophagy [42, 43]. Therefore, BNIP3 has an important role in apoptosis. We discovered that PRV infection increased BNIP3 expression to explore its role in PRV-induced apoptosis. Additionally, we demonstrated that BNIP3 upregulated apoptosis induced by PRV, and BNIP3 could increase PRV replication.

The JAK/STAT signaling pathway is an intracellular signaling pathway that responds to cytokines and growth hormones. JAK/STAT signaling pathway is intracellular signal transduction in response to cytokines and growth hormones. When JAKs activated STATs, STAT formatted active homodimers, heterodimers, or tetramers monomers through a conformational change, and the active STATs translocate into the nucleus to regulate gene expression [44-48]. Furthermore, JAK/STATs signaling pathway is implicated in autoimmune diseases and the pathogenesis of inflammatory diseases.

Nevertheless, the role of the JAK/STAT signaling pathway has not been reported in apoptosis during PRV replication. Therefore, we revealed that PRV infection upregulated JAK1 at 12, 18, and 24 hpi, as well as phospho-STAT1, phospho-STAT5, and phospho-STAT6 at 18 and 24 hpi. However, PRV infection decreased phospho-STAT3 at 18 and 24 hpi. These results demonstrated that PRV activated JAK1/STAT1, JAK1/STAT5, and JAK1/STAT6. Then, we discovered that JAK1 inhibitor Ruxolitinib decreased apoptosis induced by PRV and inhibited PRV replication.

STAT1 plays a vital role in the immune response to viral, fungal, and mycobacterium pathogens, and the STAT1 knockout leads to severe infection and rapid death of bacteria and viruses in mice [49, 50]. The JAK/STAT1 signaling pathway can inhibit HCV replication. We discovered that STAT1 knockdown increased apoptosis and PRV replication during PRV infection.

STAT3 is an important transcription factor in regulating inflammation. PRV infection inhibited phospho-STAT3, and STAT3 knockdown decreased apoptosis while inhibiting PRV replication during PRV infection. STAT3 is activated by JAKs, IL-6, IL-10, and EGF. STAT3 activation can increase Bcl-2 and Bcl-XL expressions, thereby inhibiting apoptosis. Moreover, polydatin induced MG-63 cell death via inducing apoptosis, whereas autophagy depended on STAT3 [51]. PRLR/Jak2/STAT5 contributes to prolactin-induced apoptosis by increasing the Bax/Bcl-2 ratio [52]. RP11-468E2.5 inhibits the JAK/STATs signaling pathway by targeting STAT5 and STAT6 to promote cell apoptosis in colorectal cancer cells [53]. We revealed that STAT5 knockdown downregulated PRV-induced apoptosis and inhibited PRV replication. Additionally, STAT6 upregulated PRV-induced apoptosis, as well as PRV replication.

EGCG regulates concanavalin A-induced apoptosis via JAKs/STAT3/BNIP3. EGCG downregulates JAK1 expression, thereby decreasing phospho-STAT3 to inhibit apoptosis [54]. In our study, EGCG inhibited JAK1 expression from decreasing active STAT1, whereas STAT1 knockdown increased PRV replication. Additionally, EGCG inhibited JAK1 expression from decreasing active STAT5 and STAT6, leading to BNIP3 downregulation. Nevertheless, EGCG increased phospho-STAT3 at PK15 and

PK15 B6 during PRV replication. Therefore, EGCG downregulated PRV-induced apoptosis against PRV replication depended on JAK1/STAT5 or STAT6/BNIP3 pathway (Fig. 10).

Author contributions

CRediT: Weiyin Xu, Jinghua Cheng and jianbin Wang: Data curation, Investigation, Writing - original draft, Writing - review & editing; Ping Yan: Investigation; Luyao Jiang: Formal analysis; Song Gao: Supervision, Writing - review & editing; Changchao Huan: Funding acquisition, Project administration, Supervision, Writing - review & editing.

Funding

This research was funded by the National Natural Science Foundation of China (32273015), the Jiangsu Provincial Natural Science Fund for Excellent Young (BK20220114), a project funded by the Priority Academic Program Development of Jiangsu Higher Education Institutions (PAPD), Supported by the 111 Project (D18007) and and the Top-level Talents Support Program of Yangzhou University.

Disclosure statement

The authors declare no conflicts of interest.

Data availability statement

All original data are stored in the Figshare (DOI: 10.6084/m9.figshare.33012095) under a CC - BY – 4.0 license.

References

[1] Pomeranz L. E., Reynolds A. E., Hengartner C. J. Molecular biology of pseudorabies virus: impact on neurovirology and veterinary medicine. Microbiol Mol Biol Rev, 2005, 69(3): 462-500.doi:10.1128/MMBR.69.3.462-500.2005

[2] Zhu H., Zheng C., Xing J., et al. Varicella-zoster virus immediate-early protein ORF61 abrogates the IRF3-mediated innate immune response through degradation of activated IRF3. J Virol, 2011, 85(21): 11079-11089.doi:10.1128/JVI.05098-11

[3] You H., Zheng S., Huang Z., et al. Herpes Simplex Virus 1 Tegument Protein UL46 Inhibits TANK-Binding Kinase 1-Mediated Signaling. mBio, 2019, 10(3): 10.1128/mBio.00919-19

[4] An T. Q., Peng J. M., Tian Z. J., et al. Pseudorabies virus variant in Bartha-K61-vaccinated pigs, China, 2012. Emerg Infect Dis, 2013, 19(11): 1749-1755.doi:10.3201/eid1911.130177

[5] Wang X., Wu C. X., Song X. R., et al. Comparison of pseudorabies virus China reference strain with emerging variants reveals independent virus evolution within specific geographic regions. Virology, 2017, 506: 92-98.doi:10.1016/j.virol.2017.03.013

[6] Liu Q., Wang X., Xie C., et al. A novel human acute encephalitis caused by pseudorabies virus variant strain. Clin Infect Dis, 2020, : 10.1093/cid/ciaa987

[7] Ai J. W., Weng S. S., Cheng Q., et al. Human Endophthalmitis Caused By Pseudorabies Virus Infection, China, 2017. Emerg Infect Dis, 2018, 24(6): 1087-1090.doi:10.3201/eid2406.171612

[8] Fan S., Yuan H., Liu L., et al. Pseudorabies virus encephalitis in humans: a case series study. J Neurovirol, 2020, 26(4): 556-564.doi:10.1007/s13365-020-00855-y

[9] Wang D., Tao X., Fei M., et al. Human encephalitis caused by pseudorabies virus infection: a case report. J Neurovirol, 2020, 26(3): 442-448.doi:10.1007/s13365-019-00822-2

[10] Deng X. S., Wang S., Deng A., et al. Metformin targets Stat3 to inhibit cell growth and induce apoptosis in triple-negative breast cancers. Cell Cycle, 2012, 11(2): 367-376.doi:10.4161/cc.11.2.18813

[11] Buzzai M., Jones R. G., Amaravadi R. K., et al. Systemic treatment with the antidiabetic drug metformin selectively impairs p53-deficient tumor cell growth. Cancer Res, 2007, 67(14): 6745-6752.doi:10.1158/0008-5472.CAN-06-4447

[12] Zhu Hong, Zhang Yingmei. Life and Death Partners in Post-PCI Restenosis: Apoptosis, Autophagy, and The Cross-talk Between Them. Current Drug Targets, 2018, 19(9): 1003-1008.doi:10.2174/1389450117666160625072521

[13] Djavaheri-Mergny M., Maiuri M. C., Kroemer G. Cross talk between apoptosis and autophagy by caspase-mediated cleavage of Beclin 1. Oncogene, 2010, 29(12): 1717-1719.doi:10.1038/onc.2009.519

[14] Lai I. H., Chang C. D., Shih W. L. Apoptosis Induction by Pseudorabies Virus via Oxidative Stress and Subsequent DNA Damage Signaling. Intervirology, 2019, 62(3-4): 116-123.doi:10.1159/000502047

[15] Zhou Q. Q., Shi D. S., Tang Y. D., et al. Pseudorabies virus gM and its homologous proteins in herpesviruses induce mitochondria-related apoptosis involved in viral pathogenicity. PLoS Pathogens, 2024, 20(4): e1012146.doi:ARTN e1012146
10.1371/journal.ppat.1012146

[16] Yeh C. J., Lin P. Y., Liao M. H., et al. TNF-alpha mediates pseudorabies virus-induced apoptosis via the activation of p38 MAPK and JNK/SAPK signaling. Virology, 2008, 381(1): 55-66.doi:10.1016/j.virol.2008.08.023

[17] Chang C. D., Lin P. Y., Liao M. H., et al. Suppression of apoptosis by pseudorabies virus Us3 protein kinase through the activation of PI3-K/Akt and NF-kappaB pathways. Res Vet Sci, 2013, 95(2): 764-774.doi:10.1016/j.rvsc.2013.06.003

[18] O'shea J. J., Schwartz D. M., Villarino A. V., et al. The JAK-STAT pathway: impact on human disease and therapeutic intervention. Annu Rev Med, 2015, 66(1): 311-328.doi:10.1146/annurev-med-051113-024537

[19] Chacko S. M., Thambi P. T., Kuttan R., et al. Beneficial effects of green tea: a literature review. Chin Med, 2010, 5: 13.doi:10.1186/1749-8546-5-13

[20] Mckay D. L., Blumberg J. B. The role of tea in human health: an update. J Am Coll Nutr, 2002, 21(1): 1-13.doi:10.1080/07315724.2002.10719187

[21] Sudano Roccaro A., Blanco A. R., Giuliano F., et al. Epigallocatechin-gallate enhances the activity of tetracycline in staphylococci by inhibiting its efflux

from bacterial cells. Antimicrob Agents Chemother, 2004, 48(6): 1968-1973.doi:10.1128/AAC.48.6.1968-1973.2004

[22] Weber J. M., Ruzindana-Umunyana A., Imbeault L., et al. Inhibition of adenovirus infection and adenain by green tea catechins. Antiviral Res, 2003, 58(2): 167-173.doi:10.1016/s0166-3542(02)00212-7

[23] Osada K., Takahashi M., Hoshina S., et al. Tea catechins inhibit cholesterol oxidation accompanying oxidation of low density lipoprotein in vitro. Comp Biochem Physiol C Toxicol Pharmacol, 2001, 128(2): 153-164.doi:10.1016/s1532-0456(00)00192-7

[24] Haqqi T. M., Anthony D. D., Gupta S., et al. Prevention of collagen-induced arthritis in mice by a polyphenolic fraction from green tea. Proc Natl Acad Sci U S A, 1999, 96(8): 4524-4529.doi:10.1073/pnas.96.8.4524

[25] Dona M., Dell'aica I., Calabrese F., et al. Neutrophil restraint by green tea: inhibition of inflammation, associated angiogenesis, and pulmonary fibrosis. J Immunol, 2003, 170(8): 4335-4341.doi:10.4049/jimmunol.170.8.4335

[26] Sartippour M. R., Shao Z. M., Heber D., et al. Green tea inhibits vascular endothelial growth factor (VEGF) induction in human breast cancer cells. J Nutr, 2002, 132(8): 2307-2311.doi:10.1093/jn/132.8.2307

[27] Huan C., Xu W., Guo T., et al. (-)-Epigallocatechin-3-Gallate Inhibits the Life Cycle of Pseudorabies Virus In Vitro and Protects Mice Against Fatal Infection. Front Cell Infect Microbiol, 2020, 10: 616895.doi:10.3389/fcimb.2020.616895

[28] Detection of apoptosis induced by new type gosling viral enteritis virus in vitro through fluorescein annexin V-FITC/PI double labeling. World Journal of Gastroenterology, 2008, : CNKI:SUN:ZXXY.0.2008-14-007

[29] Chen G., Ray R., Dubik D., et al. The E1B 19K Bcl-2-binding protein Nip3 is a dimeric mitochondrial protein that activates apoptosis. Journal of Experimental Medicine, 1997, 186(12): 1975-1983.doi:DOI 10.1084/jem.186.12.1975

[30] Vande Velde C., Cizeau J., Dubik D., et al. BNIP3 and genetic control of necrosis-like cell death through the mitochondrial permeability transition pore. Molecular and Cellular Biology, 2000, 20(15): 5454-5468.doi:Doi 10.1128/Mcb.20.15.5454-5468.2000

[31] Yan J., Yun H., Yang Y., et al. Upregulation of BNIP3 promotes apoptosis of lung cancer cells that were induced by p53. Biochemical and Biophysical

Research Communications, 2006, 346(2): 501-507.doi:10.1016/j.bbrc.2006.05.160

[32] Ericksen B., Wu Z., Lu W., et al. Antibacterial activity and specificity of the six human {alpha}-defensins. Antimicrob Agents Chemother, 2005, 49(1): 269-275.doi:10.1128/AAC.49.1.269-275.2005

[33] Ivashkiv L. B., Donlin L. T. Regulation of type I interferon responses. Nat Rev Immunol, 2014, 14(1): 36-49.doi:10.1038/nri3581

[34] Zhao X., Zhang E., Ren X., et al. Edaravone alleviates cell apoptosis and mitochondrial injury in ischemia-reperfusion-induced kidney injury via the JAK/STAT pathway. Biol Res, 2020, 53(1): 28.doi:10.1186/s40659-020-00297-0

[35] Deng X. S., Wang S. L., Deng A. L., et al. Metformin targets Stat3 to inhibit cell growth and induce apoptosis in triple-negative breast cancers. Cell Cycle, 2012, 11(2): 367-376.doi:10.4161/cc.11.2.18813

[36] Buzzai M., Jones R. G., Amaravadi R. K., et al. Systemic treatment with the antidiabetic drug metformin selectively impairs p53-deficient tumor cell growth. Cancer Research, 2007, 67(14): 6745-6752.doi:10.1158/0008-5472.Can-06-4447

[37] Zhu H., Zhang Y. Life and Death Partners in Post-PCI Restenosis: Apoptosis, Autophagy, and The Cross-talk Between Them. Current Drug Targets, 2018, 19(9): 1003-1008.doi:10.2174/1389450117666160625072521

[38] Djavaheri-Mergny M., Maiuri M. C., Kroemer G. Cross talk between apoptosis and autophagy by caspase-mediated cleavage of Beclin 1 (vol 29, pg 1717, 2010). Oncogene, 2010, 29(49): 6508-6508.doi:10.1038/onc.2010.514

[39] Ampomah P. B., Lim L. H. K. Influenza A virus-induced apoptosis and virus propagation. Apoptosis, 2020, 25(1-2): 1-11.doi:10.1007/s10495-019-01575-3

[40] Ohyama K., Nishina M., Yuan B., et al. Apoptosis induced by influenza virus-hemagglutinin stimulation may be related to fluctuation of cellular oxidative condition. Biol Pharm Bull, 2003, 26(2): 141-147.doi:10.1248/bpb.26.141

[41] Li M., Li J., Zeng R., et al. Respiratory Syncytial Virus Replication Is Promoted by Autophagy-Mediated Inhibition of Apoptosis. J Virol, 2018, 92(8): 10.1128/jvi.02193-17

[42] Nikoletopoulou V., Markaki M., Palikaras K., et al. Crosstalk between apoptosis,

necrosis and autophagy. Biochim Biophys Acta, 2013, 1833(12): 3448-3459.doi:10.1016/j.bbamcr.2013.06.001

[43] Maiuri M. C., Le Toumelin G., Criollo A., et al. Functional and physical interaction between Bcl-X(L) and a BH3-like domain in Beclin-1. Embo Journal, 2007, 26(10): 2527-2539.doi:10.1038/sj.emboj.7601689

[44] O'shea J. J., Kontzias A., Yamaoka K., et al. Janus kinase inhibitors in autoimmune diseases. Annals of the Rheumatic Diseases, 2013, 72 Suppl 2: ii111-115.doi:10.1136/annrheumdis-2012-202576

[45] Mao X., Ren Z., Parker G. N., et al. Structural bases of unphosphorylated STAT1 association and receptor binding. Mol Cell, 2005, 17(6): 761-771.doi:10.1016/j.molcel.2005.02.021

[46] Stark G. R., Darnell J. E., Jr. The JAK-STAT pathway at twenty. Immunity, 2012, 36(4): 503-514.doi:10.1016/j.immuni.2012.03.013

[47] O'shea J. J., Holland S. M., Staudt L. M. JAKs and STATs in immunity, immunodeficiency, and cancer. N Engl J Med, 2013, 368(2): 161-170.doi:10.1056/NEJMra1202117

[48] Myllymaki H., Ramet M. JAK/STAT pathway in Drosophila immunity. Scand J Immunol, 2014, 79(6): 377-385.doi:10.1111/sji.12170

[49] Meraz M. A., White J. M., Sheehan K. C., et al. Targeted disruption of the Stat1 gene in mice reveals unexpected physiologic specificity in the JAK-STAT signaling pathway. Cell, 1996, 84(3): 431-442.doi:10.1016/s0092-8674(00)81288-x

[50] Dupuis S., Jouanguy E., Al-Hajjar S., et al. Impaired response to interferon-alpha/beta and lethal viral disease in human STAT1 deficiency. Nat Genet, 2003, 33(3): 388-391.doi:10.1038/ng1097

[51] Jiang C. Q., Ma L. L., Lv Z. D., et al. Polydatin induces apoptosis and autophagy via STAT3 signaling in human osteosarcoma MG-63 cells. J Nat Med, 2020, 74(3): 533-544.doi:10.1007/s11418-020-01399-5

[52] De Dios N., Orrillo S., Irizarri M., et al. JAK2/STAT5 Pathway Mediates Prolactin-Induced Apoptosis of Lactotropes. Neuroendocrinology, 2019, 108(2): 84-97.doi:10.1159/000494975

[53] Jiang L., Zhao X. H., Mao Y. L., et al. Long non-coding RNA RP11-468E2.5 curtails colorectal cancer cell proliferation and stimulates apoptosis via the

JAK/STAT signaling pathway by targeting STAT5 and STAT6. J Exp Clin Cancer Res, 2019, 38(1): 465.doi:10.1186/s13046-019-1428-0

[54] Li S., Xia Y., Chen K., et al. Epigallocatechin-3-gallate attenuates apoptosis and autophagy in concanavalin A-induced hepatitis by inhibiting BNIP3. Drug Des Devel Ther, 2016, 10: 631-647.doi:10.2147/DDDT.S99420

Figure legends:

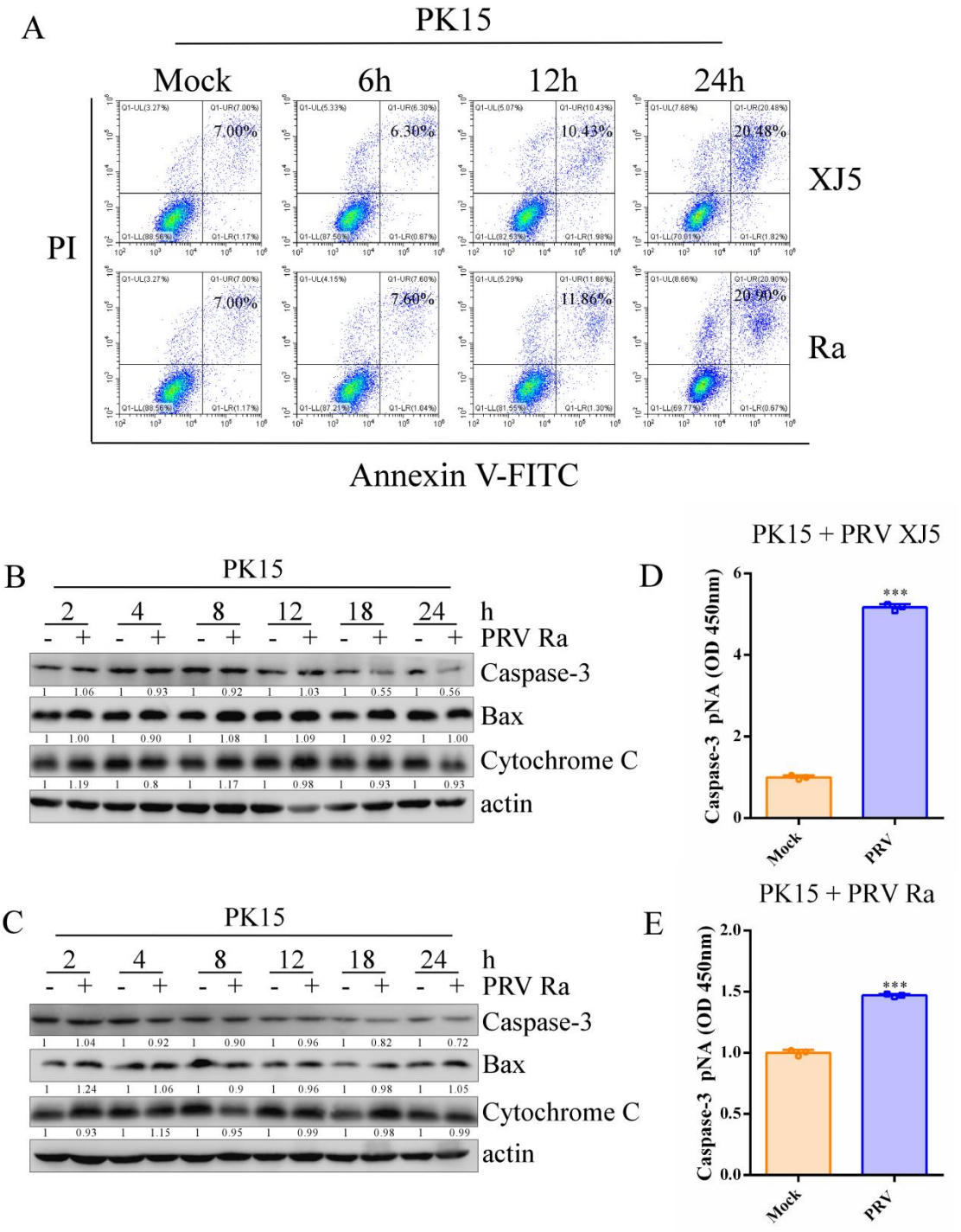


Figure 1. PRV infection-induced apoptosis via caspase-3. (A) PK15 cells were infected with PRV XJ5 and Ra (0.1 MOI) for 6, 12, and 24 h. The cells were collected for Annexin V-FITC/propidium iodide (PI) staining and flow cytometry analysis. The same cells had the same mock. (B and C) PK15 cells were inoculated with PRV XJ5 and Ra (0.1 MOI) for 2, 4, 8, 12, 18, and 24 h to examine apoptotic genes caspase-3, Bax, and

Cytochrome C using Western blot, while relative intensity was analyzed using Image J. (D and E) PK15 cells were infected with PRV XJ5 and Ra (0.1 MOI) for 24 h to determine the enzyme activity of caspase-3 via caspase-3 activity assay. The values represent the mean ± SD from three independent experiments. (* represents $P < 0.05$, ** represents $P < 0.01$, *** represents $P < 0.001$).

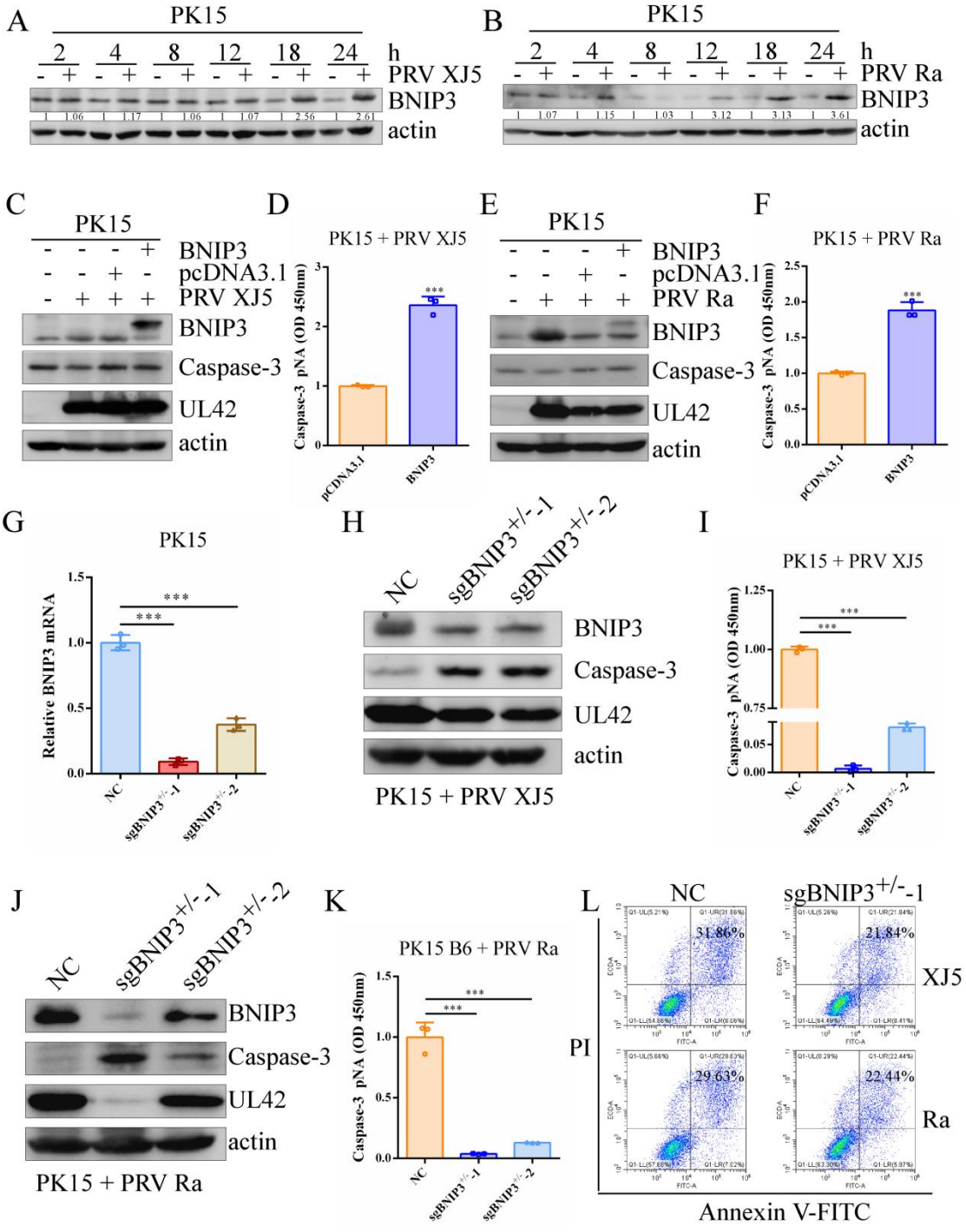


Figure 2. BNIP3 increased apoptosis depended on caspase-3. (A and B) PK15 cells

infected with PRV XJ5 or Ra for 2, 4, 8, 12, 18, and 24 h, then we collected cells to determine BNIP3 levels using Western blot analysis. (C-F) PK15 cells overexpressed BNIP3 for 24 h and were infected with PRV XJ5 or Ra for 24 h. (C and E) Western blot was used to evaluate BNIP3, caspase-3, PRV-UL42, and β-actin protein levels. (D and F) Caspase-3 enzyme activity was detected using a caspase-3 activity assay. (G) Knockout BNIP3 gene was monitored using RT-qPCR. (H-K) BNIP3-knockout PK15 cells were infected with PRV XJ5 or Ra for 24 h. (H and J) BNIP3, caspase-3, and PRV-UL42 were measured using Western blot. (I and K) The enzyme activity of caspase-3 was determined using a caspase-3 activity assay. (L) Apoptosis was analyzed using flow cytometry. The values represent mean ± SD from three independent experiments. (* represents $P < 0.05$, ** represents $P < 0.01$, *** represents $P < 0.001$).

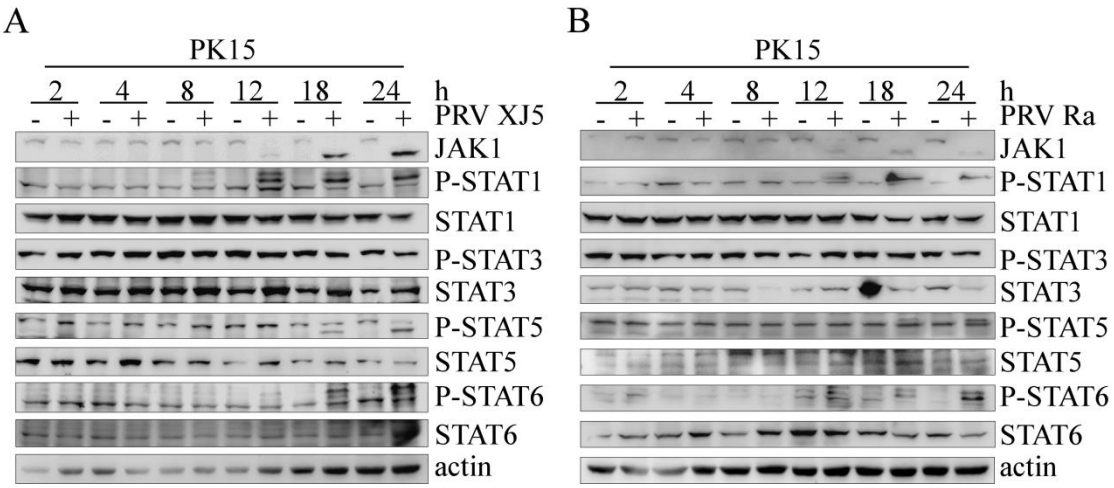


Figure 3. The effect of PRV infection on the JAK/STAT pathway. (A and B) PK15 cells were infected with PRV XJ5 or Ra (0.1 MOI) for 2, 4, 8, 12, 18, and 24 h. We collected cells to analyze the protein levels of JAK1, STAT1/3/5/6, phospho-STAT1/3/5/5 by Western blot.

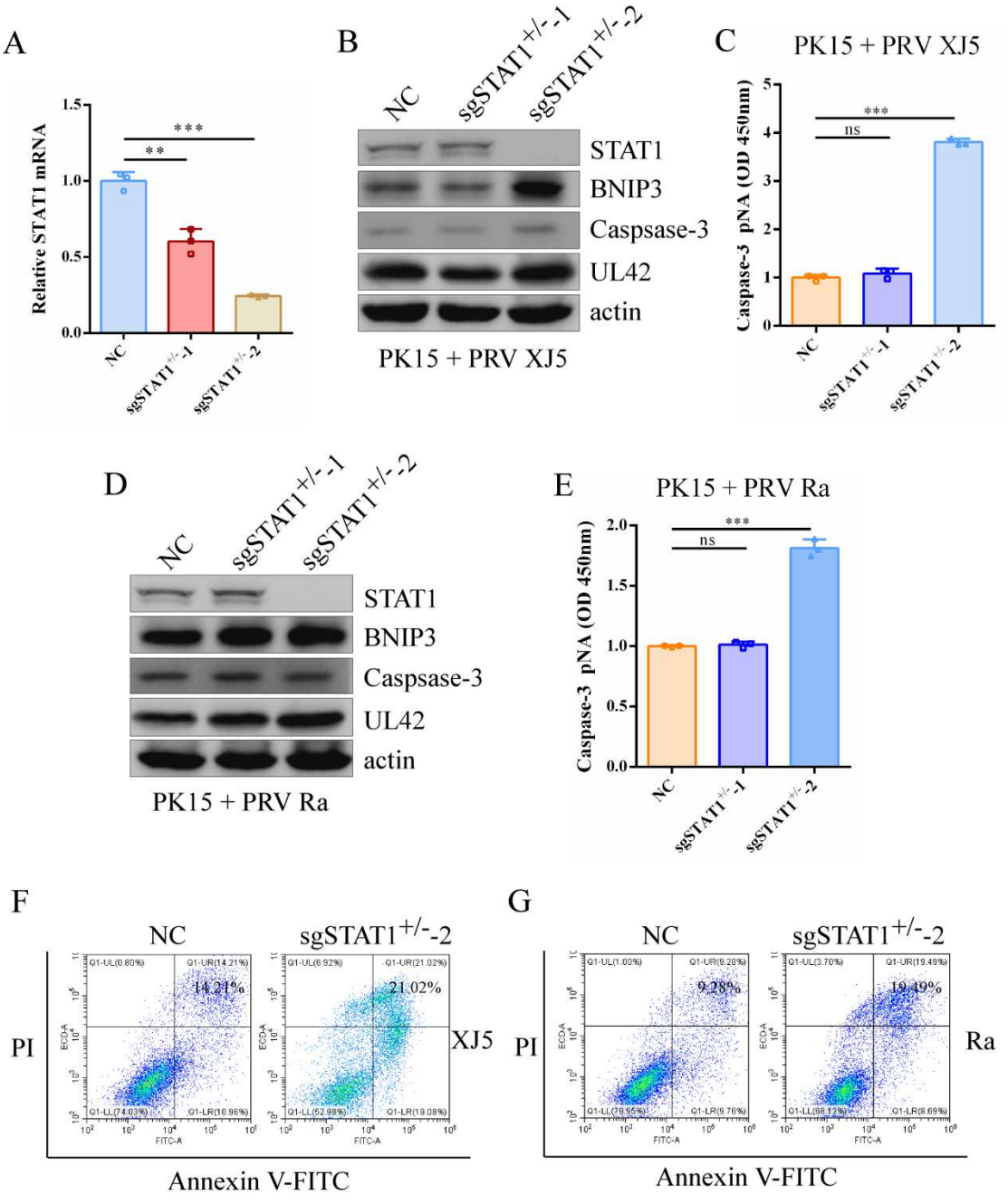


Figure 4. The effect of STAT1 on apoptosis. (A) Knockout STAT1 gene was monitored using RT-qPCR. (B-E) STAT1 knockout-PK15 cells were infected with PRV XJ5 or Ra for 24 h. (B and D) STAT1, BNIP3, caspase-3, and PRV UL42 were measured by Western blot. (C and E) The enzyme activity of caspase-3 was checked using a caspase-3 activity assay. (F and G) Following 24 h of infection with PRV XJ5 or Ra, STAT1-knockdown PK15 cells were harvested and subjected to flow cytometric analysis for apoptosis detection. The values represent mean ± SD from three independent experiments. (* represents $P < 0.05$, ** represents $P < 0.01$, *** represents $P < 0.001$).

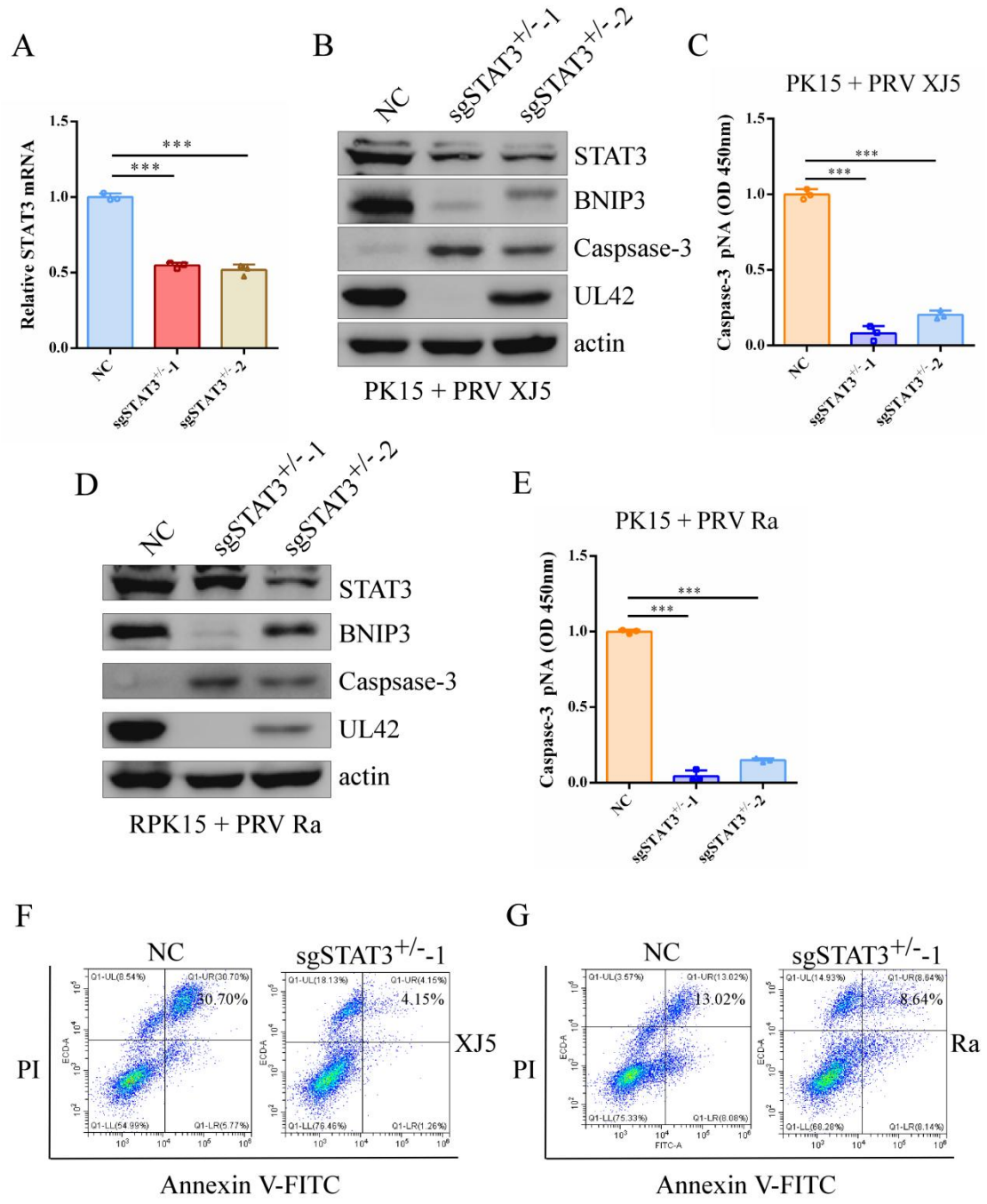


Figure 5. The effect of STAT3 on apoptosis. (A) Knockout STAT3 gene was monitored using RT-qPCR. (B-E) STAT3 knockout-PK15 cells were infected with PRV XJ5 or Ra for 24 h. (B and D) STAT3, BNIP3, caspase-3, and PRV UL42 were measured by Western blot. (C and E) The enzyme activity of caspase-3 was checked using a caspase-3 activity assay. (F and G) Following 24 h of infection with PRV XJ5 or Ra, STAT3-knockdown PK15 cells were harvested and subjected to flow cytometric analysis for apoptosis detection. The values represent mean ± SD from three independent experiments. (* represents $P < 0.05$, ** represents $P < 0.01$, *** represents $P < 0.001$).

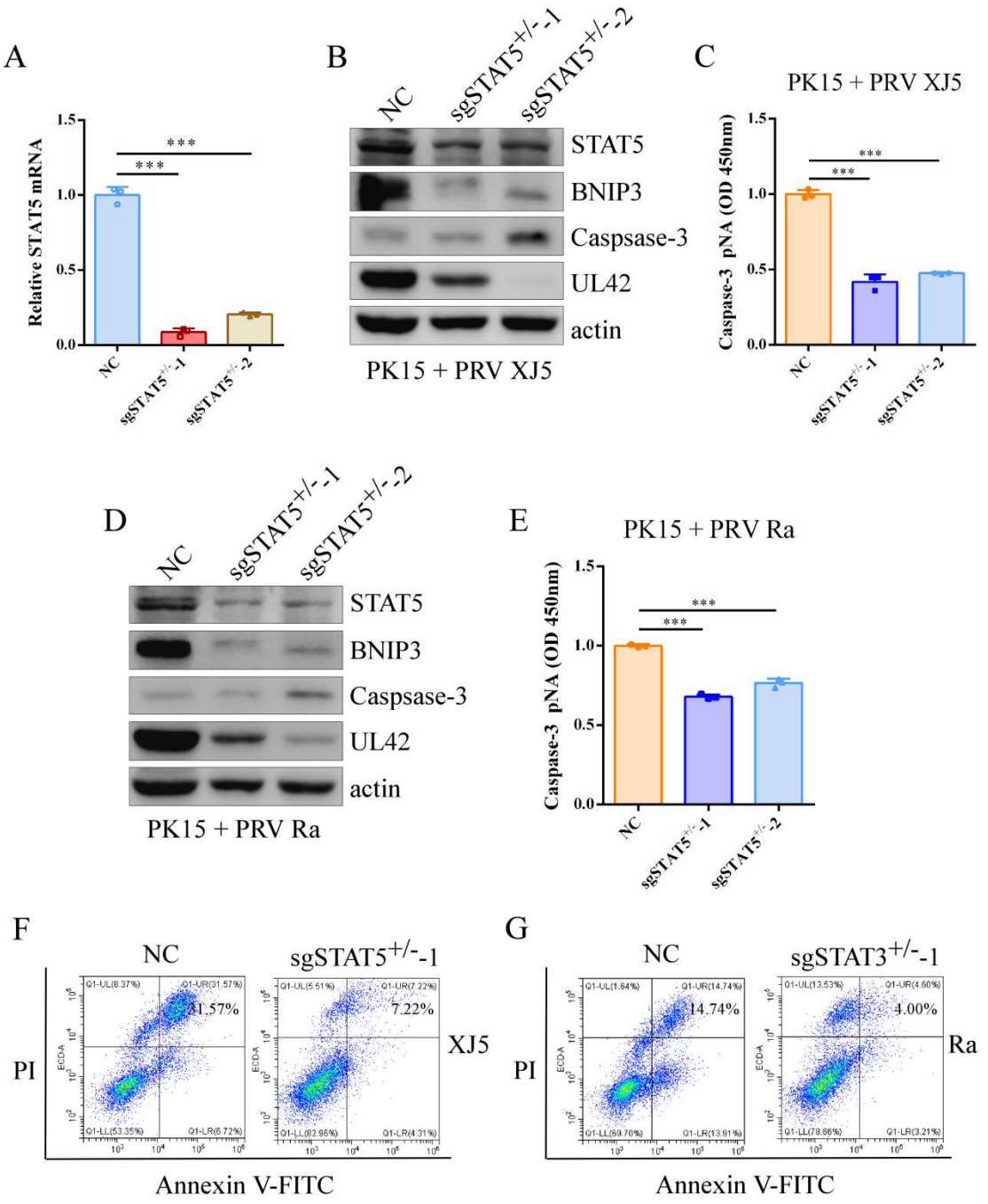


Figure 6. STAT5 knockout diminished apoptosis. (A) Knockout STAT5 gene was monitored using RT-qPCR. (B-E) STAT5 knockout-PK15 cells were infected with PRV XJ5 or Ra for 24 h. (B and D) STAT5, BNIP3, caspase-3, and PRV UL42 were measured by Western blot. (C and E) The enzyme activity of caspase-3 was checked using a caspase-3 activity assay. (F and G) Following 24 h of infection with PRV XJ5 or Ra, STAT3-knockdown PK15 cells were harvested and subjected to flow cytometric analysis for apoptosis detection. The values represent mean ± SD from three independent experiments. (* represents $P < 0.05$, ** represents $P < 0.01$, *** represents

$P < 0.001$).

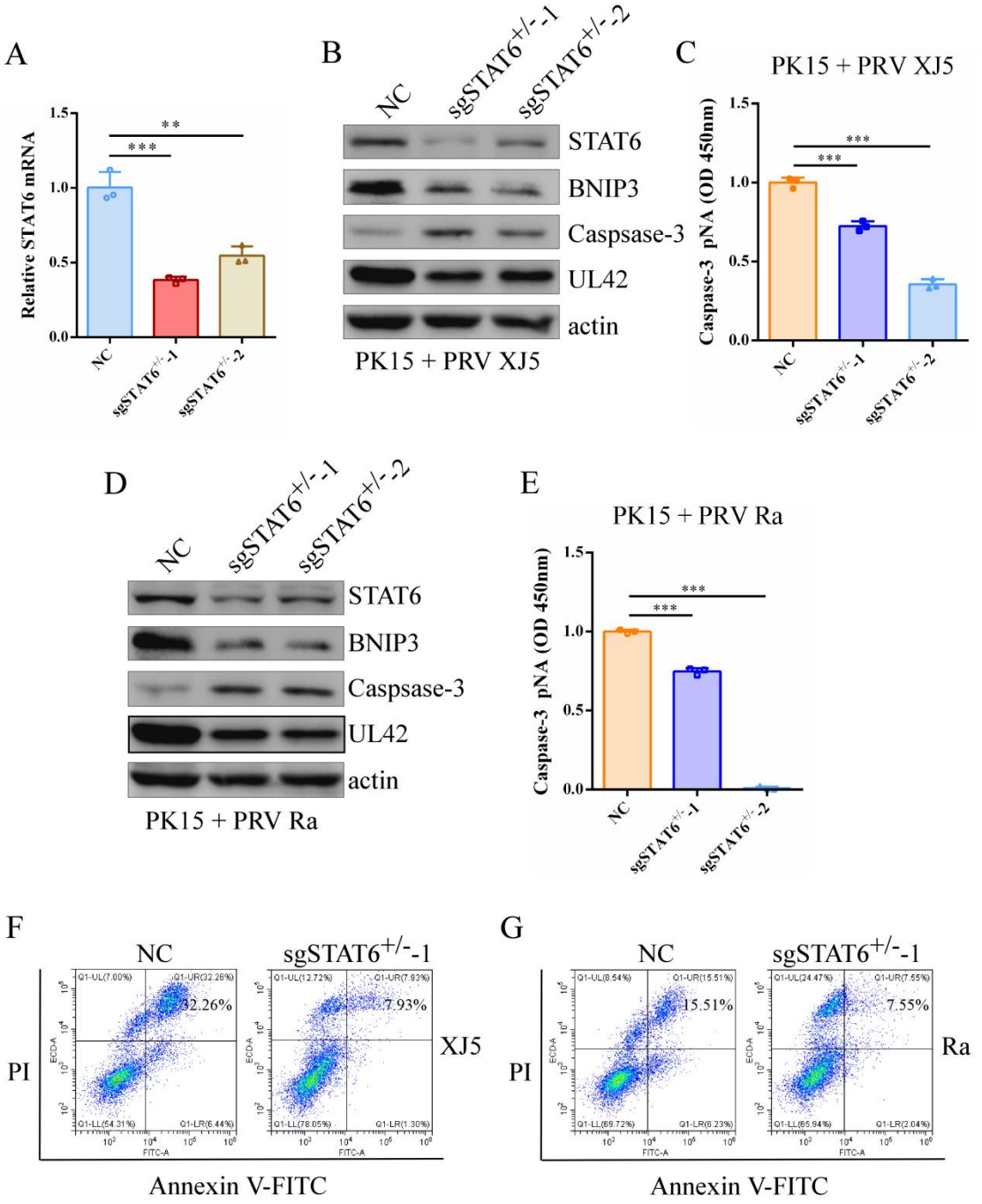
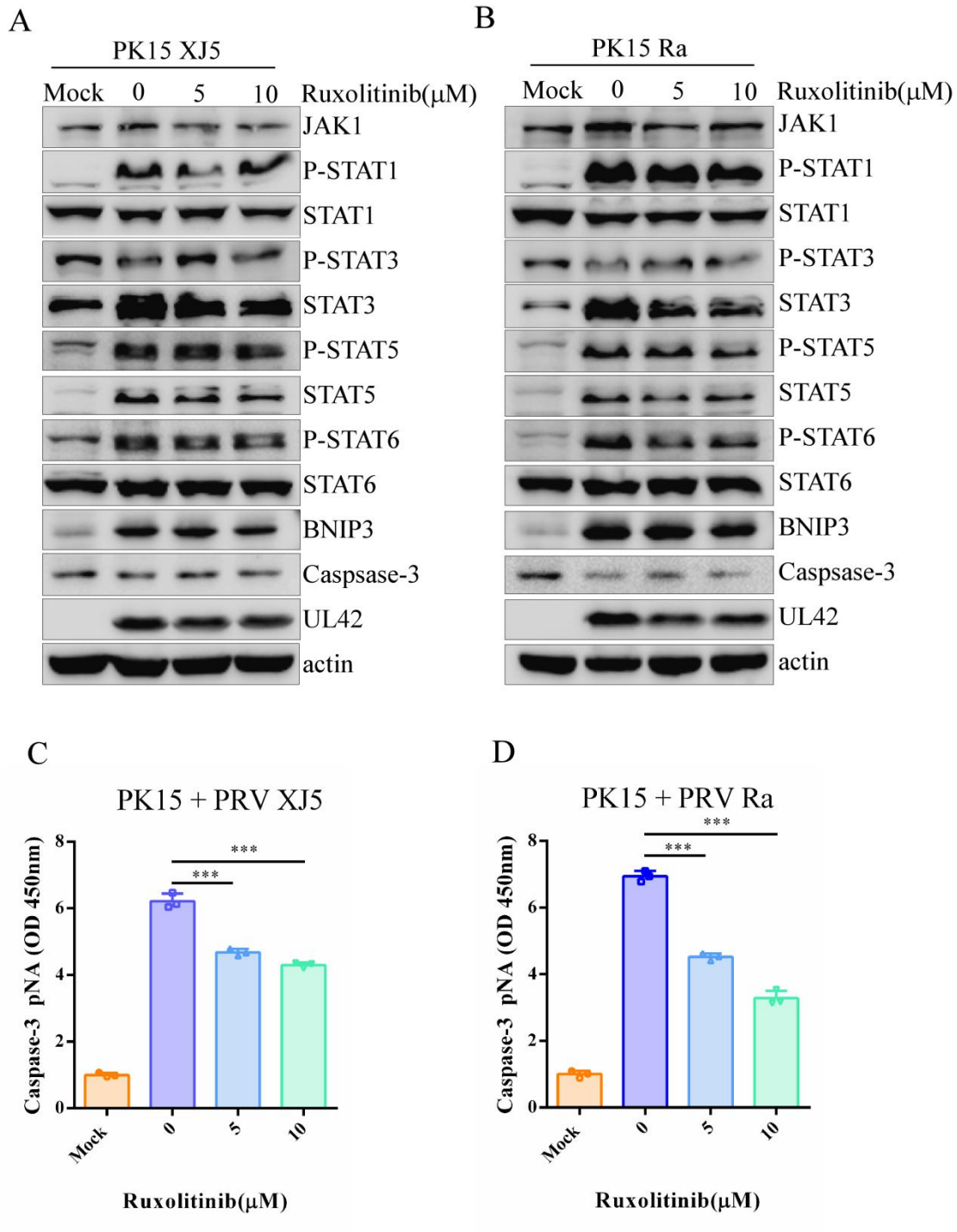


Figure 7. STAT6 knockout diminished apoptosis. (A) Knockout STAT6 gene was monitored using RT-qPCR. (B-E) STAT6 knockout-PK15 cells were infected with PRV XJ5 or Ra for 24 h. (B and D) STAT6, BNIP3, caspase-3, and PRV UL42 were measured by Western blot. (C and E) The enzyme activity of caspase-3 was checked using a caspase-3 activity assay. (F and G) Following 24 h of infection with PRV XJ5 or Ra, STAT3-knockdown PK15 cells were harvested and subjected to flow cytometric analysis for apoptosis detection. The values represent mean ± SD from three

605 independent experiments. (* represents $P < 0.05$, ** represents $P < 0.01$, *** represents
606 $P < 0.001$).



607

608 **Figure 8.** JAK1 upregulated apoptosis induced by PRV. PK15 cells were treated with
609 JAK1 inhibitor Ruxolitinib and infected with PRV XJ5 or Ra for 24 h. (A and B) JAK1,
610 STAT1/3/5/6, phospho-STAT1/3/5/6, BNIP3, caspase-3, and PRV UL42 were
611 monitored by Western blot. (C and D) Caspase-3 enzyme activity was measured using

a caspase-3 activity assay. The values represent mean ±SD from three independent experiments. (* represents $P < 0.05$, ** represents $P < 0.01$, *** represents $P < 0.001$).

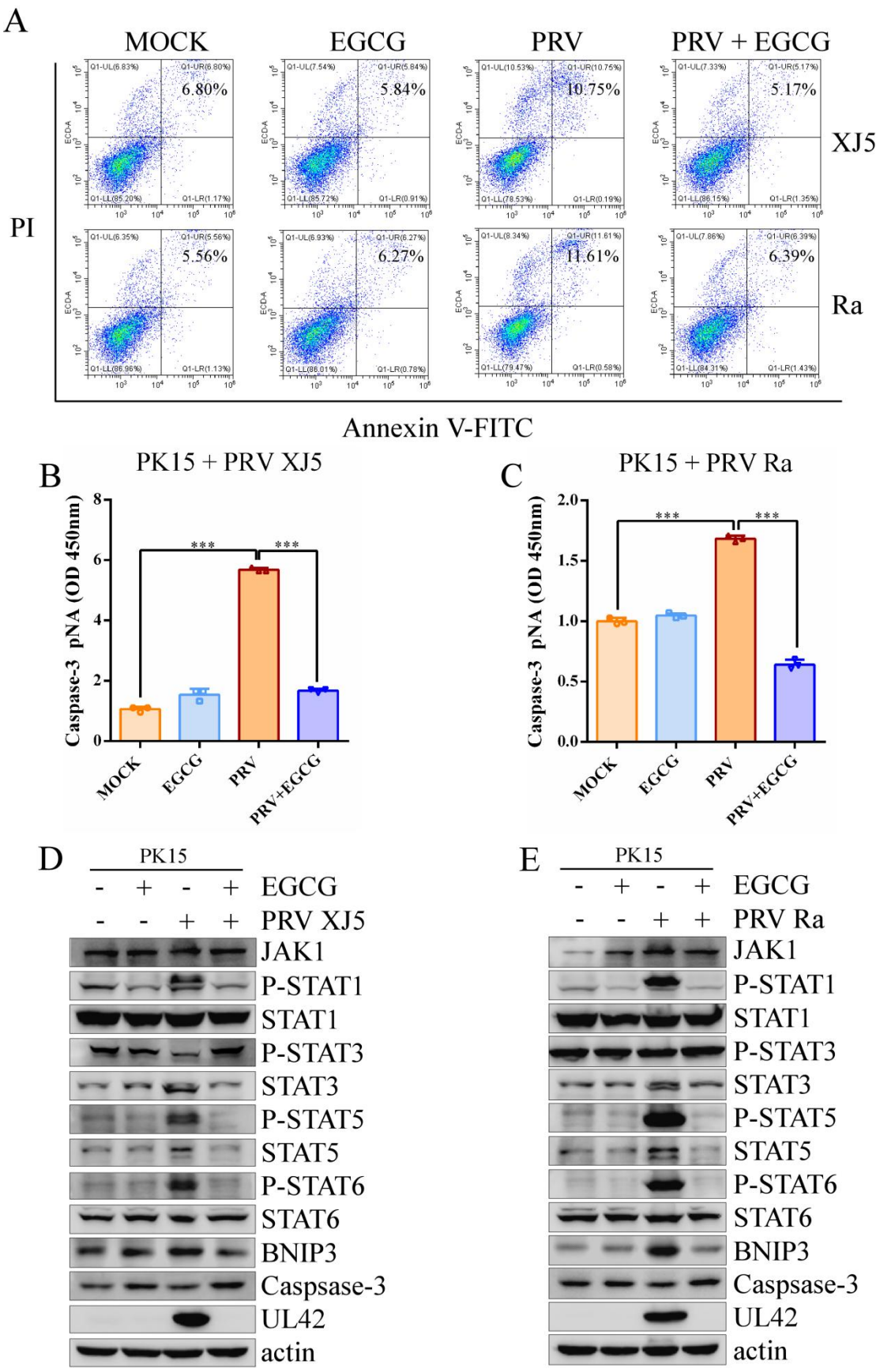
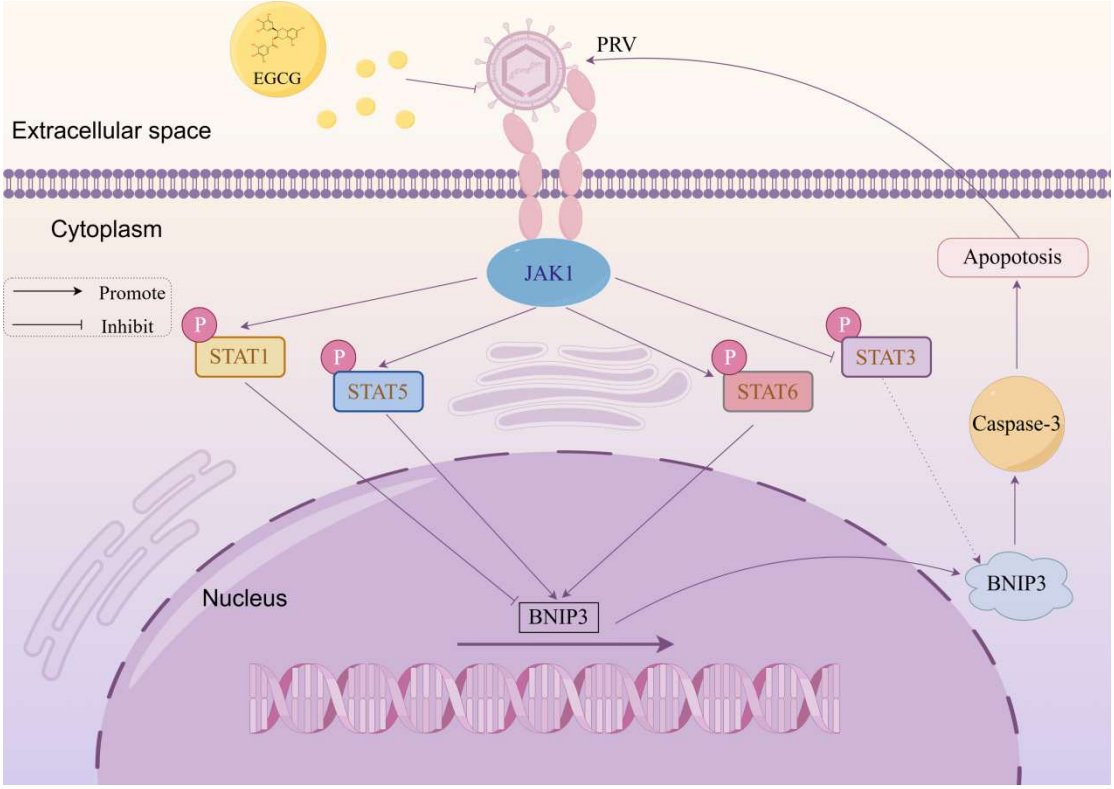


Figure 9. EGCG perturbed apoptosis induced by PRV depending on JAK1/STAT5 or STAT6 pathway. PK15 cells were pretreated with EGCG (50 μM) for 1 h before being

617 infected with PEV XJ5 or Ra (50 μM) for 24 h. (A) Apoptosis was analyzed using flow
618 cytometry. (B and C) Caspase-3 enzyme activity was monitored using a caspase-3
619 activity assay. (D and E) PK15 cells were pretreated with EGCG (50 μM) for 1 h before
620 being infected with PEV XJ5 or Ra (50 μM) for 24 h. STAT1/3/5/6, phospho-
621 STAT1/3/5/6, BNIP3, caspase-3 and PRV UL42 levels were monitored by Western blot.
622 The values represent mean ±SD from three independent experiments. (* represents $P <$
623 0.05, ** represents $P < 0.01$, *** represents $P < 0.001$).



624

625 **Figure 10.** Schematic presentation of anti-PRV mechanism of EGCG through
626 BNIP3/caspase-3-mediated apoptosis.

627

Supplementary Files

This is a list of supplementary files associated with this preprint. Click to download.

- Supp.docx